

Interaction mechanisms of near-surface quantum wells with oxidized and H-passivated AlGaAs surfaces

V. Emiliani, B. Bonanni, C. Presilla, M. Capizzi, and A. Frova
Dipartimento di Fisica, Università di Roma "La Sapienza," Roma 00185, Italy

Ying-Lan Chang, I.-Hsing Tan, and J. L. Merz
Center for Quantized Electronic Structures (QUEST), University of California, Santa Barbara, California 93106

M. Colocci and M. Gurioli
LENS Laboratory, Università di Firenze, Firenze 50125, Italy

(Received 15 September 1993; accepted for publication 25 January 1994)

The tunneling mechanism of electrons and holes to surface states from near-surface $\text{Al}_{0.3}\text{Ga}_{0.7}\text{As}/\text{GaAs}$ quantum wells has been investigated by steady-state and time-resolved photoluminescence spectroscopy, near liquid-helium temperature, of the excitonic $e1-hh1$ transition in the well. The ensemble of the data, taken over a wide range of optical excitation levels, for various values of the tunneling-barrier thickness, and before and after passivation of the surface by hydrogen, allows a description both of the details of the tunneling mechanism and of the character and behavior of relevant surface states. The main results are summarized as follows: (i) steady-state tunneling is ambipolar, namely, separate for electrons and holes, rather than excitonic; (ii) Spicer's advanced unified defect model for an oxidized GaAs surface, antisite-As donors as dominating surface traps, provides an appropriate description of the state distribution at the interface between AlGaAs and its oxide; (iii) hole accumulation in surface states, resulting from the nominally different unipolar tunneling probability for the two carriers (and increasing with excitation level), generates a dipole electric field across the tunneling barrier, extending into the well; (iv) hydrogenation efficiently passivates electron trapping in surface states, but not hole tunneling and the consequent generation of a surface field by illumination; (v) the experimental findings agree with a model for ambipolar tunneling based on a self-consistent quantum-mechanical approach.

I. INTRODUCTION

The tunneling of electrons and holes to surface states (SS), with consequent loss in the radiative efficiency of a quantum well (QW) formed in the immediate vicinity of the oxidized surface of the semiconductor structure, has been the object of recent investigations.¹⁻⁶ Such phenomena are of some importance in the optical and transport behavior of a variety of nanometric structures and devices, where the small separation among the parts leads to appreciable interaction of the well states among themselves and with nearby states at surfaces and interfaces.

Tunneling from QWs to surface states, followed by rapid nonradiative recombination, is a process that, for a high-quality barrier material, e.g., $\text{Al}_{0.3}\text{Ga}_{0.7}\text{As}$ in Ref. 3, sets on very sharply for surface-barrier thickness $b \sim 120 \text{ \AA}$, making the optical emission from the well virtually equal to zero for b less than 50 \AA . For defected barriers, e.g., lattice-mismatched QWs,^{4,7} tunneling can initiate for thicker surface barriers, probably due to multistep processes capable of relaxing the condition that the quantum levels in the well be aligned with the appropriate SS for tunneling to take place (multistep tunneling cannot be ruled out, of course, even in high-quality barrier material).

The QW-to-SS tunneling mechanism resembles to some extent the one known for asymmetric double QWs (ADQW).⁸⁻¹⁵ At high excitation,^{9,13} a large enough steady-state carrier density becomes available in the QWs, so as to

permit accumulation of the faster tunneling electrons in the wider well, with development of a dipole field across the barrier. The dipole layer adjusts itself so as to oppose electron tunneling and favor hole tunneling to a final ambipolar regime. A recent work demonstrates the importance of an electric field in controlling the tunneling mechanism by means of experiments done under external bias.¹⁵

The well-to-surface tunneling mechanism is less straightforward; as a consequence, although in nanodevices it may have great importance, it has not received equal attention. There are of course some close similarities. For instance, a self-consistent quantum calculation,¹⁶ based on a model distribution of SS and an infinite surface recombination velocity, proves that charge accumulation in the surface states occurs, to warrant equal electron and hole tunneling currents, which implies fields of order 10^5 V/cm . The basic difference from well-to-well tunneling is that the concentration of states where electrons and holes tunnel can be very different for the two carriers.

The rate equations for recombination via excitons in QWs are (taking different initial state for tunneling and recombination, as the experiment will later demonstrate):

$$\frac{dn}{dt} = G - J_{\text{tunn},e} - F, \quad (1a)$$

$$\frac{dp}{dt} = G - J_{\text{tunn},h} - F, \quad (1b)$$

$$\frac{dv}{dt} = F - v/\tau_{\text{recomb}}, \quad (1c)$$

where n , p , and v are the electron, hole, and exciton numbers per unit area at time t , respectively, G the generation current density, F the exciton formation current, τ_{recomb} the recombination time, and $J_{\text{tunn},e} = n/\tau_{\text{tunn},e}$, $J_{\text{tunn},h} = p/\tau_{\text{tunn},h}$ the tunneling currents, with $\tau_{\text{tunn},e}$ and $\tau_{\text{tunn},h}$ the corresponding characteristic times, inclusive of the quantum mechanical tunneling time and of the SS densities available to electrons and holes, respectively. Equations (1a), (1b), written for steady-state conditions, give

$$n/\tau_{\text{tunn},e} = p/\tau_{\text{tunn},h} = J_{\text{tunn}}, \quad (2)$$

i.e., a single value for the electron and hole tunneling current (ambipolar tunneling). For this to be possible, as $\tau_{\text{tunn},e}$ and $\tau_{\text{tunn},h}$ are in principle different, the steady-state density of electrons n and holes p in QW1 must be correspondingly unequal. This is what gives origin to dipole charge accumulation and an electric field across the barrier. The field, in turn, affects the tunneling time of carriers in opposite ways, favoring the slower ones, so that a detailed-balance condition is finally reached (this being, of course, a function of the excitation level in the well). It is worthwhile noting that the effects of tunneling and field buildup are related, but for the latter to occur tunneling of one carrier alone is sufficient. If it were possible to passivate only SS available for tunneling of one type of carrier, e.g., the electron, under optical pumping of the well, surface recombination would be blocked, but a dipole field across the barrier would develop anyway.¹⁶

The purpose of the present work is to analyze the tunneling mechanism that causes short circuiting of radiative recombination in the AlGaAs/GaAs near-surface QW, and to prove that it does not imply tunneling of the exciton as a whole, but rather separate electron and hole processes. We intend to bring support, through study of the dependence of tunneling on optical excitation in the near-surface QW and on the passivation of surface defects by hydrogen, to our model¹⁶ predicting charge buildup in surface states to warrant ambipolar tunneling, and to the advanced unified defect model (AUDM) for the AlGaAs/oxide interface, based on a dominant As-antisite defect, which pins the surface Fermi level ~ 0.75 eV above valence band.

In Sec. II we describe the experimental approach based on the investigation of QWs separated from the surface by barriers of varying thickness. Both continuous wave (cw) and time-resolved photoluminescence (PL) spectra will be measured near liquid-helium temperature, with the laser power density varied over several orders of magnitude. Section III is devoted to the experimental spectra and to the derivation of the relevant parameters. In Sec. IV we discuss the experimental data, confirming the blocking effect of hydrogen on surface recombination, with the persistence, however, of the field-induced red shift of the QW excitonic emission upon increasing excitation. The ensemble of the results indicates that tunneling to surface states, as internally produced by the presence of near-surface quantum wells, is a promising alternative tool for the investigation of surface and interface properties.

TABLE I. Set of samples used in the experiment (in the sample name, the number represents the surface-barrier thickness b , V stands for virgin, H for hydrogenated). The given values of τ_{rise} and τ_{decay} , respectively, the PL rise and the decay times, correspond to an average pulse power $\sim 10^3$ W/cm².

Sample name	Barrier thickness b (Å)	H-dose ions/cm ²	τ_{rise} (ps)	τ_{decay} (ps)
350V	350	...	70	125
80V	80	...	90	140
60V	60	...	50	150
30V	30	...	50	110
120H ^a	120	10^{16}	90	130

^aHydrogenated sample with nonradiative centers in QW1 fully passivated due to in-diffusion of H over a 10-month aging period.

II. EXPERIMENT

The starting structure comprises two Al_{0.3}Ga_{0.7}As/GaAs QWs grown on a nonintentionally doped (100) GaAs substrate by molecular beam epitaxy (MBE). Due to residual C impurities, both GaAs and AlGaAs are lightly p -type doped. An upper QW (called hereafter QW1), 60 Å in width, is separated from the surface by a 350-Å-thick AlGaAs layer. A second QW (called hereafter QW2), 100 Å in width, is separated from QW1 by a 3500 Å AlGaAs layer. The deeply embedded well is insensitive to surface states and is used as a reference for normalization of luminescence intensity, so as to minimize small inhomogeneity effects in samples cut from the same wafer. Different pieces of material were then etched in an appropriate citric-acid/hydrogen-peroxide solution in order to achieve surface-barrier thicknesses that appeared of particular significance: (1) 80 Å, where the exciton recombination current and the tunneling current were in the ratio $\sim 1:1$; (2) 60 Å, ratio $\sim 1:10$; and (3) 30 Å, ratio $\sim 1:100$. The above surface-barrier thicknesses were estimated approximately by interpolating, for equal excitation levels, the emission vs surface barrier curve published earlier for the same materials structure.³ After etching, prior to measurements the samples were exposed to air in order to grow an oxide layer. For a useful comparison, two more samples were investigated along with the newly produced ones: (4) a 120-Å-thick barrier hydrogenated sample, showing no tunneling effects and the highest radiative efficiency among all explored samples;⁶ and (5) a 350-Å-thick barrier sample, used as a standard reference, which presents no evidence of interaction between QW1 and surface states.

The first four samples were derived from a single initial chip, split into very small parts. The last sample, coming from a different zone of the same wafer, did not present strictly identical spectral characteristics, its $e1-hh1$ free-exciton emission in QW1 being accompanied by a weak bound-exciton shoulder at lower energy. Since such discrepancies were reasonably well reproduced in the emission of QW2, the integrated normalized QW1/QW2 photoluminescence (called hereafter NPL) virtually cancels any effect of wafer inhomogeneities. A summary of the characteristics of the investigated samples, and their labels used in the text, is given in Table I, along with the main parameters to be deduced later from the analysis of the experimental data.

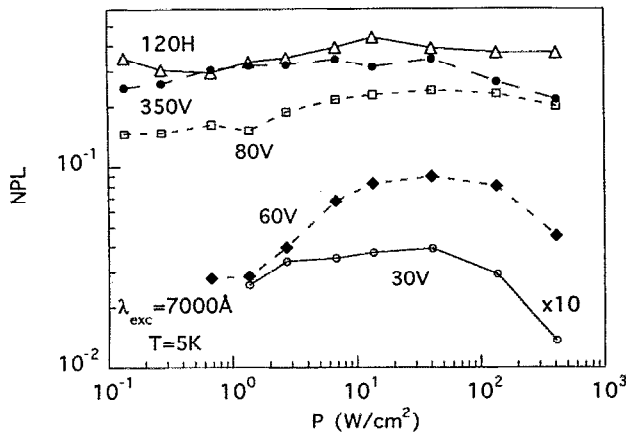


FIG. 1. Normalized cw photoluminescence NPL from the $e1-hh1$ exciton in QW1 for samples with different surface-barrier thickness (given in Å by the number in sample name) as a function of excitation power density. H stands for hydrogenated sample, V for virgin, naturally oxidized sample. The data for sample 30V have been amplified ten times.

cw-PL measurements were carried out at liquid-helium temperature, using a Ti-sapphire laser to avoid carrier generation in the AlGaAs barrier material (excitation wavelength 7000 Å, vs 6300 Å corresponding to the $Al_{0.3}Ga_{0.7}As$ band gap). Spectra of emitted radiation corresponding to the $e1-hh1$ excitonic transition in both the near-surface QW1 and the deeply embedded QW2 were analyzed by means of a GaAs-cathode photomultiplier. The data are mostly given in the normalized form, i.e., ratio between the integrated emissions from QW1 and QW2.

PL rise and decay times at the peak of the $e1-hh1$ exciton emission band were measured by pumping with a dye laser (excitation wavelength between 7300 and 7650 Å), which generated 6-ps-long pulses with a repetition rate of 76 MHz; a streak camera was used for detection.

Hydrogenation of the material was achieved at room temperature with a Kaufman ion source, operated at 100 eV with a diameter of the ion beam uniform over the sample area. The current density was of order $10 \mu A/cm^2$. The background pressure of the chamber was $\sim 10^{-6}$ mbar and the total pressure, after introduction of H, $\sim 4.10^{-4}$ mbar, with a H-ion flow of ~ 60 standard cubic centimeters per second. The total H-ion dose impinging on the sample surface was estimated by monitoring the current and carefully reproduced (this dose is of course much larger than the actual number of incorporated particles).

III. RESULTS

A. cw photoluminescence

NPL, normalized cw photoluminescence, of the various samples is shown in Fig. 1 as a function of laser power density. We see that the no tunneling, hydrogenated sample 120H, which has also undergone full passivation of deep defect centers inside QW1 because of H in-diffusion during aging,⁶ has the highest radiative efficiency, comparatively constant with power density. The recombination time τ_{recomb} in this case is virtually coincident with the radiative lifetime

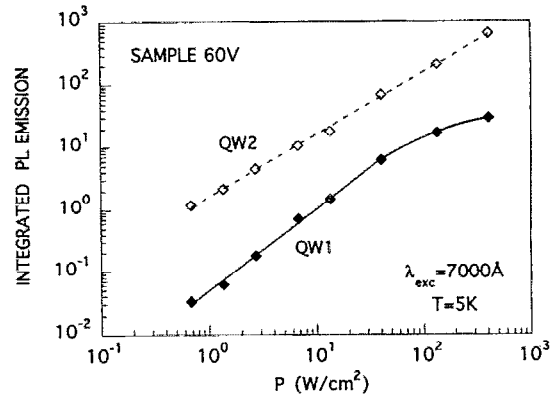


FIG. 2. Virgin sample 60V (60-Å-thick surface barrier): separate plot, vs power density P , of the integrated $e1-hh1$ excitonic emissions from QW1 (slope 1.3 in the low-power range) and QW2 (slope 1 throughout).

τ_{rad} . The radiative efficiency of the reference sample 350V, not interacting with the surface,³ is only slightly lower than the above.

Samples 80V, 60V, and 30V, in the order, present an increasingly lower NPL signal, and also a more marked dependence on laser power. This effect is entirely ascribable to QW1, as illustrated in Fig. 2, where the integrated emissions of QW1 and QW2 of sample 60V are separately plotted to

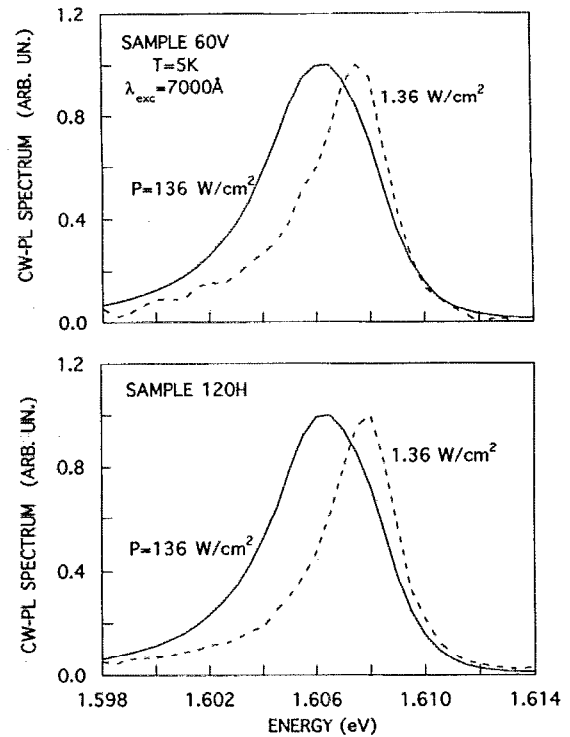


FIG. 3. cw-PL spectral emission of the $e1-hh1$ exciton in QW1 for virgin sample 60V and hydrogenated sample 120H, for medium-low and high laser excitation. Despite the absence of tunneling in the latter case, the red shift and the line broadening for increasing power are virtually equal for the two samples.

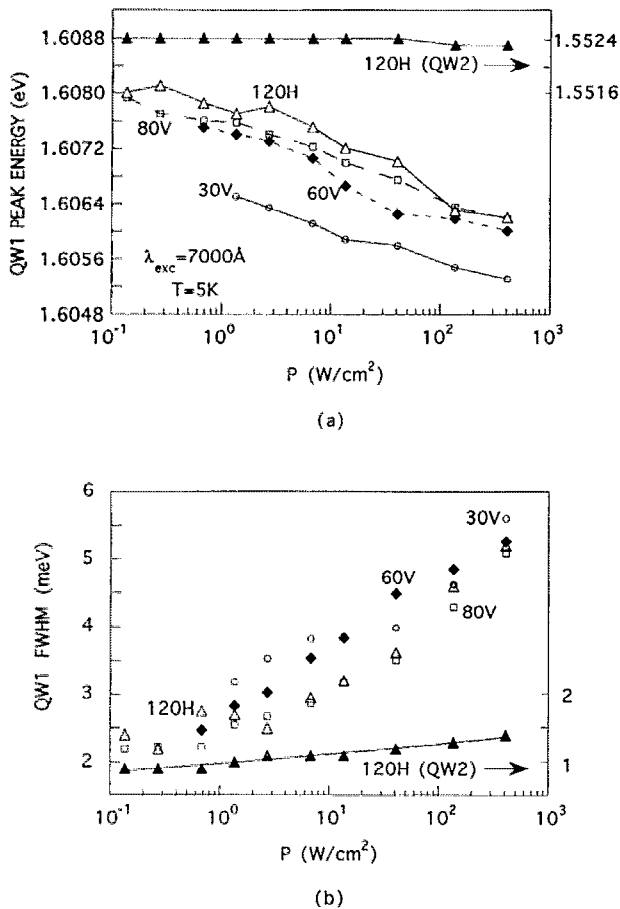


FIG. 4. (a) Shift of the energy position for the $e1-hh1$ excitonic peak in QW1 of virgin samples as a function of laser power density P . The shift is observed also in the hydrogenated sample 120H, having no ambipolar tunneling and surface recombination, but not in the deeply embedded QW2, shown for comparison. (b) Full width at half maximum (FWHM) of the $e1-hh1$ excitonic peak in QW1 of virgin samples as a function of laser power density P . The behaviors of QW1 and QW2 in sample 120H are shown for comparison.

demonstrate the strict linearity of the latter against the remarkable superlinearity of the former in the low-power range and the bending over at high excitation.

The ratio between the *normalized* ambipolar tunneling current to surface states

$$NJ_{\text{tunn}} = \text{NPL}_{120H} - \text{NPL} \quad (3)$$

and the normalized recombination current NPL in QW1 changes from about 1 to 100, in going from sample 80V to sample 30V. Due to the complex interplay between available states for tunneling, and the insurgence of an electric field across the surface barrier, with unequal populations of electrons and holes in QW1, the power dependence of the tunneling current is not the same for low and high values of surface-barrier thickness. Note that for high tunneling efficiency, samples 30V and 60V, small changes in tunneling show up as large variations in QW1 radiative emission, indicative of the high sensitivity of the method.

The development of an electric field across the barrier, and its tailing in QW1, is proven by the experimental observation of a red shift of the $e1-hh1$ excitonic recombination

peak, due to the quantum confined Stark effect,¹⁷ and its gradual broadening with increasing excitation inside the well. This is illustrated in Figs. 3 and 4(a), 4(b). All samples with a near-surface well, including 120H, the passivated one, present a shift increasing more or less linearly with the logarithmic power density. The shift is larger for samples with stronger tunneling, seeming particularly important for sample 30V. QW1 in reference sample 350V (not shown) presents no shift, nor does QW2 in any of the samples [see, as a typical example, QW2 for sample 120H in Fig. 4(a)]. Figure 4(b) illustrates the simultaneous effect of line broadening, which again is nearly absent in sample 350V (not shown) and in all QW2s (see again sample 120H).

From Eqs. (1) in steady-state conditions ($i=1,2$ is the QW index),

$$F_i = G_i - J_{i,\text{tunn}}, \quad (4a)$$

$$\nu_i = F_i \tau_{i,\text{recomb}}, \quad (4b)$$

with $F_2 = G_2$ and $J_{2,\text{tunn}} = 0$. It follows, for the PL intensities,

$$\text{PL}_i = k_i \nu_i / \tau_{i,\text{rad}} = k_i F_i \tau_{i,\text{recomb}} / \tau_{i,\text{rad}}, \quad (4c)$$

where k_i accounts for the detection efficiency due to the experimental configuration. From Eqs. (4), we obtain, for $\tau_{2,\text{recomb}} \sim \tau_{2,\text{rad}}$ and $G_1 = G_2 = G$, and putting $F_1 = F$,

$$\text{NPL} = \text{PL}_1 / \text{PL}_2 = (k_1 \tau_{1,\text{recomb}}) / (k_2 \tau_{1,\text{rad}}) F / G. \quad (4d)$$

The exciton formation current F , relative to the $e-h$ pair generation current G , is shown in Fig. 5. The strong drop in NPL when the barrier thickness is reduced results either from the decrease in exciton formation current F , or the decrease in exciton recombination efficiency, caused by tunneling to SS.

B. Time-resolved photoluminescence

The decay time τ_{decay} for excited carriers in QW1 has been measured directly by time-resolved PL, using typically an excitation wavelength of 7560 Å and always tuning the monochromator at the peak of the $e1-hh1$ excitonic transition. Typical time-resolved profiles for the various samples

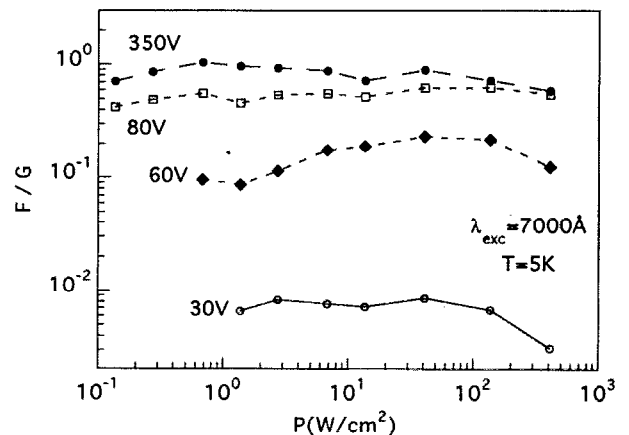


FIG. 5. Formation current F of recombining excitons, in units of G , for virgin samples of different surface-barrier thickness, as a function of laser power-density P .

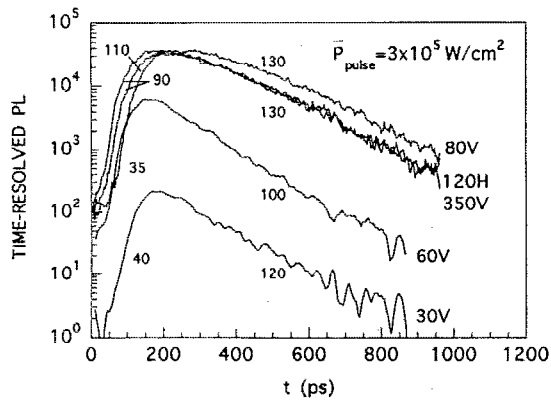


FIG. 6. Time-resolved PL at 10 K and $\lambda_{exc} = 7560 \text{ \AA}$, of the $e1-hh1$ excitonic peak, in virgin samples of varying surface-barrier thickness and, for comparison, in the hydrogenated sample 120H. The rise and decay times shown are given in ps.

are shown in Fig. 6. The power dependence of the rise and decay times, as determined through fittings of the curves in Fig. 6 by a function $B [\exp(-t/\tau_{decay}) - \exp(-t/\tau_{rise})]$, is given in Figs. 7(a) and 7(b); typical values are also listed in Table I. It is worthwhile anticipating here (see discussion in Sec. IV C) (i) that the exciton decay time is virtually independent of the occurrence of tunneling, which means that the exciton as a whole does not tunnel and that the drop in NPL is due to the decrease in exciton formation current F ; (ii) that the attainment of the maximum exciton emission occurs with a remarkable delay with respect to the laser pulse (not an instrumental effect, since observed risetimes span over a wide range).

C. Passivation by hydrogen

After samples were studied in their virgin form, they were exposed to room-temperature hydrogen treatment. For an impinging dose of 10^{14} cm^{-2} , no important change in behavior was observed. For a higher dose, namely, $4 \times 10^{15} \text{ cm}^{-2}$, QW1 of samples 80V and 60V shows a very good recovery of its radiative efficiency, confirming earlier results.³ Emission from sample 30V, instead, remains very low. It appears as if the conditions of the oxide, thickness, presence of defects, etc., play a basic role in determining the passivation of interface defects. Further detailed analysis is in progress and will be reported in a forthcoming paper.

IV. DISCUSSION

A. Surface-state distribution

The dramatic drop in cw-PL reported in Ref. 3 for thin barriers, a factor 100 over a factor 3 in surface-barrier thickness (we recall that pumping occurs only in the QWs), is immediately indicative of a tunneling mechanism.

Let us consider the widely accepted picture for the distribution of surface states in oxidized GaAs surfaces (advanced unified defect model, AUDM),¹⁸ believed to hold also for GaAlAs. The natural oxidation of the surface does create, at the interface, an extended layer of heavily dis-

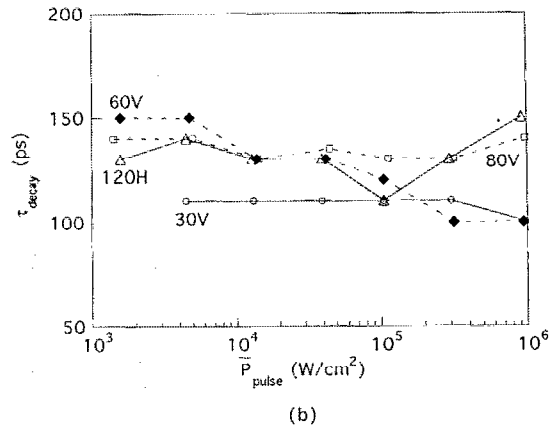
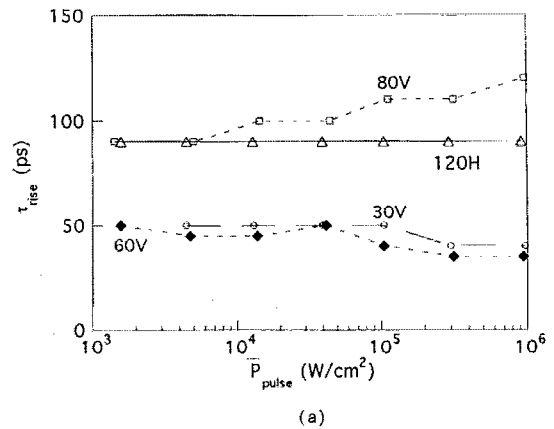


FIG. 7. (a) Rise time of the $e1-hh1$ fundamental exciton level, in virgin samples of varying surface-barrier thickness and in hydrogenated sample 120H, as a function of average laser-pulse power. (b) Decay time of the $e1-hh1$ fundamental exciton level, in virgin samples of varying surface-barrier thickness and in hydrogenated sample 120H, as a function of average laser-pulse power. Data in (a) and (b) are deduced from best fittings of curves in Fig. 6 in terms of the difference of two exponentials, and are known with an uncertainty of 10 ps. ($\lambda_{exc} = 7560 \text{ \AA}$, $T = 10 \text{ K}$).

rupted material,¹⁹ where surface-like states are possibly found at all energies, somewhat reminiscent of the case of amorphous GaAs. Nevertheless, the defect with the highest concentration is believed to be^{18,20,21} antisite arsenic As_{Ga} , a double donor with one level (neutral, D^0/D^+) at $\sim 0.75 \text{ eV}$ above the valence band and one (singly charged, D^+/D^{2+}) at $\sim 0.5 \text{ eV}$ above the valence band.^{22,23} In an oxidized surface, the As_{Ga} defect is dominant as a consequence of the initial formation of the thermodynamically unstable²⁴ oxide As_2O_3 and of the ensuing reaction²¹



Experiments show that the energy of such levels is the same in AlGaAs, and independent of Al concentration.²⁵

The surface conceivably presents a certain number of compensating antisite Ga_{As} centers, double acceptors in the bulk material with a level at 0.08 (neutral) and 0.2 eV (singly charged).²⁶ All the above defect levels, due to the highly disordered character of the interfacial region, are expected to

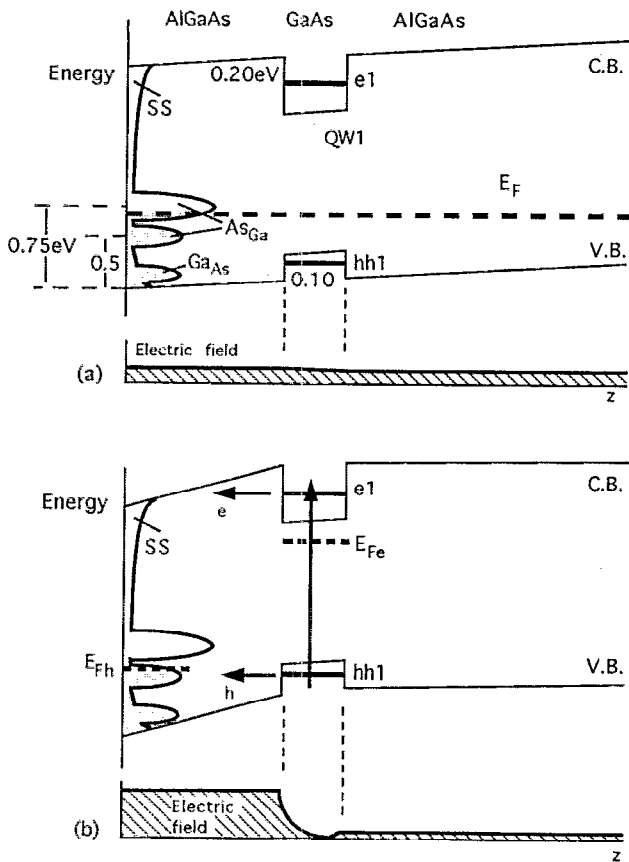


FIG. 8. (a) Scheme of the band structure and density of surface states for the near-surface QW structure (QW1) in equilibrium conditions. Continuous exponential Urbach tails extend into the gap. The surface Fermi level E_F is pinned within the upper band of the As-antisite defect. The net charge in SS is positive. The electric-field profile is also shown (field value of order 10^4 V/cm). (b) Scheme of the band structure, density of surface states, quasi-Fermi levels, and electric-field profile under high cw excitation of QW1. The field in the barrier is of order 10^5 V/cm. The field below QW1 is virtually screened.

be spread in energy over a few tenths of an eV, the Ga_{As} doublet showing up probably as a single band, very close to the valence states.

By pinning the Fermi level within the upper band of the As_{Ga} defect,²⁷ we have the schematic equilibrium condition shown in Fig. 8(a), where the bulk Fermi level has been taken, at liquid-He temperature, near the top of the valence band, as for a residual p doping with carbon, and the band tilting extends all the way to the other end of the (nearly insulating) AlGaAs structure. In such conditions, the value of the equilibrium electric field is at most 2×10^4 V/cm, corresponding to a net positive charge in SS $\sim 1.5 \times 10^{11}$ cm⁻². This would cause only a small potential drop over the surface barrier, in our case ≤ 100 Å. The $hh1$ level in the QW is lined up, therefore, with a high-density quasi continuum of states containing electrons where, under pumping, holes can tunnel [see Fig. 8(b)].

Contrary to holes, Fig. 8(b) shows that electrons do not have an easy path to reach the main recombination level, i.e., the As_{Ga} defect: from the $e1$ state, they must first tunnel to surface or barrier states of low density, possibly to the conduction-band continuum, then decay to the deep As_{Ga}

bands. In the present picture, the holes are therefore the “easy” carriers, the tunneling current being limited by the behavior of electrons.

In spite of the nearly infinite surface recombination velocity, which makes the quasi-Fermi level for electrons at the surface remain close to its equilibrium position, the quasi-Fermi level for holes is gradually lowered when pumping in QW1 is increased, with consequent enhancement of the positive charge in surface states. To explain the superlinear radiative recombination in QW1, illustrated in Figs. 1 and 2 at low power, we must admit that this process is accompanied by an initial reduction of the available states for tunneling, either for holes or for electrons, or for both.

In an analogous but opposite way, the large drop in PL occurring at pumping power densities above 40 W/cm², very conspicuous in the high-tunneling 30V sample, can be ascribed to an increase in tunneling current, possibly due [see Fig. 8(b)] to the narrowing of the triangular barrier for electrons to tunnel into conduction-band levels, forbidden in principle, but experimentally observed.¹¹ Instead, an explanation in terms of lengthening of the radiative lifetime, due to quantum confined Stark effect, is to be ruled out because in narrow wells the effect is hardly detectable,²⁸ as confirmed by our own decay time data in Fig. 7(b). A more detailed understanding of the tunneling mechanism will come from the discussion of time-resolved spectra in Sec. IV C.

In light of what follows, it is important to stress that the absence of steady-state tunneling in sample 120H is strictly a consequence of the hydrogen treatment. Prior to hydrogenation, but also after annealing in vacuum at about 300 °C, it gave clearcut evidence of ambipolar tunneling effects.^{3,6}

B. The field profile

Let us discuss in more detail the magnitude and the behavior of the electric field that builds up across the surface barrier under optical pumping, with tailing inside QW1. Figures 4(a) and 4(b) indicate that the field magnitude is controlled by the generation rate of carriers in QW1, though the tunneling rate also comes into play (for equal pumping, the red shift and the broadening increase monotonically in going from sample 120H, no tunneling, to 30V, highest tunneling). It is important to stress that the shift always has the same sign, suggesting that the field does not invert from the initial condition [Fig. 8(a)], simply getting larger and larger with pumping. This is a further argument in support of the starting idea that the tunneling probability is nominally higher for holes.

To make some estimates, let us fix the attention on sample 60V, with 90% of the total recombination occurring at the surface. The maximum shift ΔE_p observed in the PL emission peak is about 2 meV, see Fig. 4(a). For an empirical relationship, grossly deduced from data in Ref. 28, $\Delta E_p = CL_z^3 E^{3/2}$, where $C = 4.1 \times 10^{-13}$ meV Å⁻³ (V/cm)^{-3/2}, L_z is the well width, and E is the field, this shift corresponds to a mean electric field in QW1 of about 8×10^4 V/cm. The largest full width at half maximum (FWHM), more than 5 meV [see Fig. 4(b)], gives a measure of the field nonuniformity inside the well, due to photocarrier screening, with a peak value at the well boundary, and therefore inside the

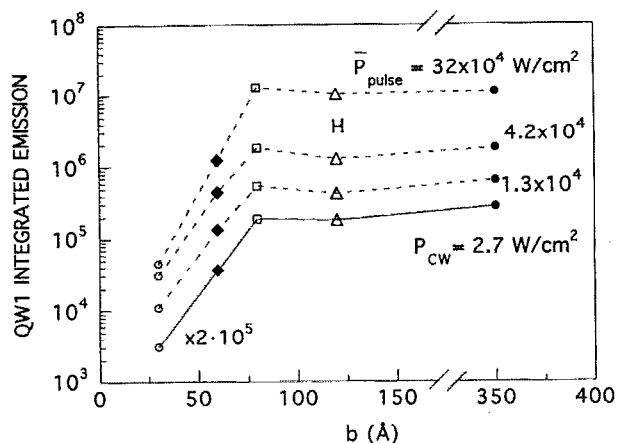


FIG. 9. Plot of the time-integrated emission of QW1 from data of Fig. 6, for three values of average laser-pulse power P . The abscissa is the surface-barrier thickness. A close correspondence is found with the energy-integrated cw-PL data.

barrier, roughly equal to 1.3×10^5 V/cm, i.e., almost twice the mean value. The field profile is schematically shown in Fig. 8(b). For a 60-Å-thick barrier, the potential drop across it is only of order 0.1 eV at the highest field achieved, even less for a thinner barrier.

The above figures are quite consistent with an estimate of the Debye length in the well. The field across the barrier, $\mathcal{E} = 1.3 \times 10^5$ V/cm, corresponds to a density of charged surface states $N_{ss} = \mathcal{E} \epsilon \epsilon_0 / q \sim 1 \times 10^{12}$ cm $^{-2}$. An equal density of mobile carriers of opposite sign is present in the well, and is attracted to the surface-barrier boundary. The excited steady-state carrier pairs in the well, for power of 400 W/cm 2 and a 1% light absorption in the well, 29 is $\sim 10^9$ cm $^{-2}$ even for the largest PL lifetime observed. Therefore the Debye length at 5 K is determined by the magnitude of N_{ss} and is equal to 5 Å, quite smaller than the width of QW1. Due to the orders-of-magnitude lower number of holes present in the well, the field in the AlGaAs layer below QW1 is almost fully screened, as illustrated in Fig. 8(b).

C. Decay-time measurements: ambipolar tunneling

The rise and decay times of the excitonic $e1-hh1$ line, respectively shown in Figs. 7(a) and 7(b), shed light on the details of the tunneling mechanism. The decay times are nearly the same for all samples, spanning from 100 and 150 ps over the entire set of samples and measurements, irrespective of the amount of tunneling. This result is fully contrasting with the behavior reported for ADQWs by Nido *et al.* 30 No particularly meaningful trend with power density is observed. In spite of the nearly constant decay-time values for the different samples, the emission intensity diminishes in the same way as the cw-PL. This is illustrated for three values of power density in Fig. 9, where the data are plotted versus surface-barrier thickness, and compared with the energy-integrated cw emission from QW1.

This behavior demonstrates three fundamental facts:

(i) Tunneling out of QW1 must take place, otherwise

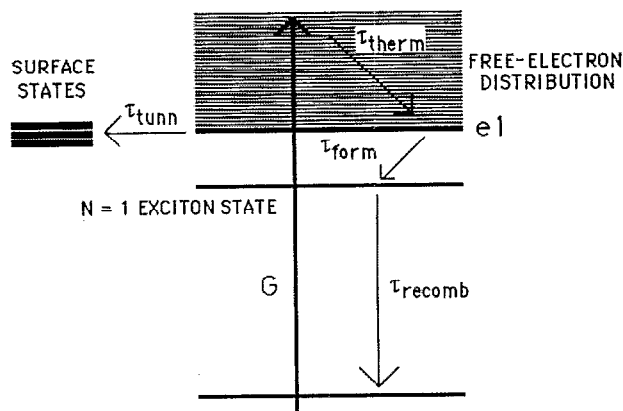


FIG. 10. Scheme of competing mechanisms of electron tunneling to surface states and excitonic recombination in QW1. The thermalization time of free carriers τ_{therm} is assumed to be much shorter than both τ_{form} , the time for an electron to fall in an excitonic state capable of recombination, and τ_{tunn} , the tunneling lifetime.

transient radiative recombination would not drop sharply when the barrier is made thinner, much in the same way as cw-PL.

(ii) Tunneling to surface states occurs basically from the free-carrier levels, i.e., prior to the formation of an excitonic complex suitable to undergo recombination. Once electrons and holes are bound in such a complex, they recombine radiatively regardless of earlier decay channels that may have been operating.

(iii) The required field for ambipolar tunneling does not build up: an average 6-ps-long pulse power, e.g., of 5×10^3 W/cm 2 , generates 10^9 cm $^{-2}$ $e-h$ pairs inside the well. However, in the previous paragraph we have shown that, for ambipolar tunneling to occur, a three-orders-of-magnitude larger carrier density is required.

We now wish to make a few additional considerations about points (i) and (ii) above. We draw first, see Fig. 10, a schematic picture of the recombination and tunneling mechanisms. We know, on the basis of experiment, that the only decay to the equilibrium state is radiative via the fundamental excitonic level (i.e., $\tau_{\text{recomb}} \cong \tau_{\text{rad}} \cong \tau_{\text{decay}}$, the measured decay time). A quantitative expression for the time-resolved data of Figs. 6 and 9, far enough from the laser pulse, is of type

$$I(t) = K \text{NPL} \exp(-t/\tau_{\text{decay}}),$$

where $I(t)$ is the emission intensity, K is a constant, NPL is the normalized cw-PL, and τ_{decay} for all samples stays around the value 130 ps, measured in sample 120H, where surface recombination is absent. This would not be so, either if appreciable tunneling of the exciton as a whole were possible, or if excitons, after forming, could be reionized. The latter process in a narrow QW is negligible even at fields $\sim 10^5$ V/cm, 28 on the other hand, experimental evidence that exciton tunneling does not occur in ADQWs is available. 31 This is even more plausible for tunneling to surface states: discrete exciton levels cannot exist in the vicinity of the surface, the well-known “dead layer” of depth of order the classical

exciton Bohr radius³² ($\sim 130 \text{ \AA}$ in AlGaAs, i.e., larger than all tunneling barriers used in the present experiment). Recent data, moreover, demonstrate that the behavior of excitons, even in wider barriers, is well described by separate confinement of electrons and holes, with subsequent inclusion of the Coulomb interaction.³³

D. Rise time

The problem of exciton formation and relaxation in a GaAs QW has been thoroughly discussed in recent papers.^{31,34–36} Formation times of the complex close to 20 ps have been reported. However, Damen *et al.*³⁶ have measured PL zero-to-peak times up to 300 ps, corresponding to rise times of 100–150 ps, the same as ours for no tunneling. The effect was explained in terms of formation of excitons with large total momentum K in times not larger than 20 ps (corresponding to motion in the parallel planes), and subsequent slow thermalization to the $K=0$ singlet state, the only one where coupling with radiation can take place. We refer to Roussignol *et al.*³⁵ for a detailed discussion of the excitation energy and density dependence of the relaxation to the bottom of the heavy-hole exciton band.

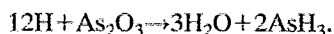
The rise times we report in Fig. 7(a) are deduced by fitting the experimental data in Fig. 6 with the function $B [\exp(-t/\tau_{\text{decay}}) - \exp(-t/\tau_{\text{rise}})]$. In a separate publication¹⁶ we will show that such a functional relation is quite appropriate in the limit for tunneling currents dominating over the exciton formation current. If this is the case, the risetime is given by $[1/\tau_{\text{tunn},e} + 1/\tau_{\text{tunn},h}]^{-1}$. In the opposite limit, tunneling currents negligible with respect to the exciton formation current, the above fitting function can still be employed, but with a different meaning for τ_{rise} , which approaches the value of τ_{decay} .

This behavior compares quite well with the fitting results shown in Table I. In particular we have $\tau_{\text{rise}} \leq 50 \text{ ps}$ in highly tunneling samples 30V and 60V, while $\tau_{\text{rise}} \cong \tau_{\text{decay}}$ in samples where radiative recombination is important.

E. Effect of hydrogenation

We recall that in cw-PL the electric field develops both in samples that exhibit steady-state tunneling and in the hydrogenated 120H no tunneling sample. This can be explained by a passivation by hydrogen of only one kind of surface defects, those responsible for tunneling of electrons. Holes build up the dipole field, but surface recombination is blocked.

Heavy H treatment of oxidized GaAs surfaces, in particular at high temperature, leads to removal of As^{37,38} through the reaction³⁹



Actually, not only the hydrogen-treated area becomes As deficient, but also contains minute Ga particles.³⁸ It is worth mentioning that also experiments dealing with the clean GaAs free surface indicate that hydrogenation tends to produce a highly disordered, Ga-rich surface region.^{40–43} As mentioned in Sec. III C, hydrogen passivation in our case is done very mildly, at room temperature, with a minimal dose

of low-energy ions (100 eV). The fact that hole tunneling is hardly affected seems to rule out that removal of As, at least from its antisite positions, is of some importance. An alternative explanation, whereby As_{Ga} is removed but novel defects related to excess Ga are equally effective in hole tunneling, seems less plausible (this is suggested by the notion that, for sulphur treatments, As_{Ga} is more efficiently passivated than Ga_{As}, with inversion of their concentration ratio and lowering of the Fermi-level pinning).^{19,21,44}

At low H doses, one might also consider the possibility of the formation of a stable H-As-H complex at antisite-As atoms, theoretically expected.⁴⁵ This would imply passivation for hole tunneling, since efficient deactivation by hydrogen of EL2 centers in the bulk is a well established result.⁴⁶ This mechanism lends itself to the same kind of criticism applied above to the effect of As removal from the surface.

Finally, it is a safe fact that H blocks electron tunneling. The surface band structure [Fig. 8(b)] does not present specific defects for them to tunnel to. Their getting to the surface for recombination with holes at the As_{Ga} defect is made possible through multiple-step processes via centers in the barrier and/or at the surface. Residual shallow donors, next to the bottom of the conduction band, are most likely to be involved in such path. It is well known that many donors are readily passivated by hydrogen, so this may be the cause for the blocking of electron tunneling. The mechanism of differential passivation of surface states for electron and hole tunneling, however, is still far from being understood and this is ground for more systematic investigation through different surface treatments and annealing processes.

V. CONCLUSIONS

The main result of this investigation, where tunneling from near-surface QWs to surface states in Al_{0.3}Ga_{0.7}As/GaAs multistructures is analyzed by monitoring the stationary and time-resolved radiative emission from the well under a variety of experimental conditions, is a clearcut demonstration that tunneling occurs separately for electrons and holes prior to their binding in the exciton complex which undergoes radiative recombination. In stationary conditions, due to the nominally different tunneling probabilities for the two carriers, ambipolar tunneling is achieved by the onset of a dipole electric field across the tunneling barrier, which tails into the optically excited well, as demonstrated by the red shift and the broadening of the excitonic $e1-hh1$ transition in the near-surface QW. The results are consistent with a picture of the surface-state distribution which favors hole tunneling, despite their larger mass in the three-dimensional material. The advanced unified defect model (AUDM), proposed by Spicer's group for oxidized GaAs surfaces, where antisite-As donors pin the Fermi level and act as the dominant hole-capturing surface defects, provides a very satisfactory framework to explain the observations of the present study. This suggests that carrier tunneling to surface defects from QWs may be a promising alternative tool for surface investigation, both in clean, naturally oxidized, and specially treated surfaces and interfaces. Time-resolved photoluminescence spectra have also allowed a comparative study of the two processes, formation of radiative excitons, basically oc-

curing over times in the range 50–100 ps and ambipolar tunneling, as well as a determination of the radiative recombination time for the exciton state, falling around 130 ps for all samples, irrespective of the surface-barrier thickness and therefore of the amount of tunneling taking place. Understanding of the detailed mechanism of surface passivation by hydrogen, though confirmed to be very efficient in the elimination of detrimental recombination at the surface, needs further, much more focused, experimental research.

ACKNOWLEDGMENTS

The authors are indebted to P. Chiaradia, C. Coluzza, A. Fasolino, F. Martelli, L. Pavesi, and Y.-H. Zhang for useful conversations. The work has been supported mainly by MURST (Ministry of University and Research), CNR (National Research Council) and by INFM (Consorzio Physics of Matter).

- ¹R. M. Cohen, M. Kitamura, and Z. M. Fang, *Appl. Phys. Lett.* **50**, 1675 (1987).
- ²J. M. Moison, K. Elcess, F. Houzay, J. Y. Marzin, J. M. Gerard, F. Barthe, and M. Bensoussan, *Phys. Rev. B* **41**, 12945 (1990).
- ³Y.-L. Chang, I.-H. Tan, Y.-H. Zhang, J. L. Merz, E. Hu, A. Frova, and V. Emiliani, *Appl. Phys. Lett.* **62**, 2697 (1993).
- ⁴Y.-L. Chang, M. Krishnamurthy, I.-H. Tan, E. Hu, J. L. Merz, P. Petroff, A. Frova, and V. Emiliani, *J. Vac. Sci. Technol. B* **11**, 1702 (1993).
- ⁵Z. Sobiesierski, D. I. Westwood, H. Fujikura, T. Fukui, and H. Hasegawa, *J. Vac. Sci. Technol. B* **11**, 1710 (1993).
- ⁶A. Frova, V. Emiliani, M. Capizzi, B. Bonanni, Y.-L. Chang, Y.-H. Zhang, and J. L. Merz, *SPIE* 1985, 601 (1993).
- ⁷Y. Baltagi, C. Bru, A. Tabata, T. Benyattou, S. Monéger, A. Georgakilas, K. Zekentes, G. Halkias, M. Gendry, V. Drouot, and G. Hollinger, *SPIE* 1985, 433 (1993).
- ⁸R. Sauer, T. D. Harris, and W. T. Tsang, *Surf. Sci.* **196**, 388 (1988).
- ⁹R. Sauer, K. Thonke, and W. T. Sang, *Phys. Rev. Lett.* **61**, 609 (1988).
- ¹⁰T. Tada, A. Yamaguchi, T. Ninomiya, H. Uchiki, T. Kobayashi, and T. Yao, *J. Appl. Phys.* **63**, 5491 (1988).
- ¹¹T. B. Norris, X. J. Song, W. J. Schaff, L. F. Eastman, G. Wicks, and G. A. Mourou, *Appl. Phys. Lett.* **54**, 60 (1989).
- ¹²Ph. Roussignol, A. Vinattieri, L. Carraresi, M. Colocci, and A. Fasolino, *Phys. Rev. B* **44**, 8873 (1991).
- ¹³C. Tanguy, B. Deveaud, A. Regreny, D. Hulin, and A. Antonetti, *Appl. Phys. Lett.* **58**, 1283 (1991).
- ¹⁴M. Gurioli, J. Martinez-Pastor, M. Colocci, C. Deparis, B. Chastaingt, and J. Massies, *Phys. Rev. B* **46**, 6922 (1992).
- ¹⁵R. Ferreira, P. Rolland, Ph. Roussignol, C. Delalande, A. Vinattieri, L. Carraresi, M. Colocci, N. Roy, B. Sermage, J. F. Palmier, and B. Etienne, *Phys. Rev. B* **45**, 11782 (1992).
- ¹⁶C. Presilla, A. Frova, and V. Emiliani (unpublished).
- ¹⁷J. A. Brum and G. Bastard, *Phys. Rev. B* **31**, 3893 (1985); D. A. B. Miller, D. S. Chemla, T. C. Damen, A. C. Gossard, W. Wiegmann, T. H. Wood, and C. A. Burrus, *ibid.* **32**, 1043 (1985); L. Viña, E. E. Mendez, W. I. Wang, L. L. Chang, and L. Esaki, *J. Phys. C* **20**, 2803 (1987); L. Viña, R. T. Collins, E. E. Mendez, W. I. Wang, L. L. Chang, and L. Esaki, *Springer Proceedings in Physics*, Vol. 25 (Springer, Berlin, 1988), p. 230.
- ¹⁸W. E. Spicer, Z. Liliental-Weber, E. Weber, N. Newman, T. Kendelewicz, R. Cao, C. McCants, P. Mahowald, K. Miyano, and I. Lindau, *J. Vac. Sci. Technol. B* **6**, 1245 (1988).
- ¹⁹C. J. Spindt and W. E. Spicer, *Appl. Phys. Lett.* **55**, 1653 (1989).
- ²⁰T. T. Chiang, C. J. Spindt, W. E. Spicer, I. Lindau, and R. Browning, *J. Vac. Sci. Technol. B* **6**, 1409 (1988).
- ²¹C. J. Spindt and W. E. Spicer, *Proceedings of SOTAPOCS XII* (1990), Vol. 90-15, p. 3, and references therein.
- ²²E. R. Weber, H. Ennen, V. Kaufmann, J. Windscheif, J. Schneider, and T. Wosinski, *J. Appl. Phys.* **53**, 6140 (1982); E. R. Weber and J. Schneider, *Physica B* **116**, 398 (1983).
- ²³The former level probably is involved in the well known EL2 center in bulk material [G. A. Baraff, M. Lannoo, and M. Schlueter, *Phys. Rev. B* **38**, 6003 (1988); J. Dabrowski and M. Scheffler, *ibid.* **40**, 10391 (1989)]. This point is still controversial. For a discussion of the actual configuration of the As-antisite defect, e.g., possibility of relaxed configurations, see, for instance, D. J. Chadi, *Mater. Sci. Forum* **83–87**, 447 (1992), and references therein. See also J. Dabrowski and M. Scheffler, *ibid.*, p. 735, and references therein.
- ²⁴G. P. Schwartz, G. J. Gualtieri, J. E. Griffith, and B. Schwartz, *J. Electrochem. Soc.* **128**, 410 (1981).
- ²⁵M. Fockele, B. K. Meyer, J. M. Spaeth, M. Heuken, and K. Heime, *Phys. Rev. B* **40**, 2001 (1989).
- ²⁶B. V. Shanabrook, W. J. Moore, and S. G. Bishop, *J. Appl. Phys.* **59**, 2535 (1986).
- ²⁷Y.-M. Xiong, P. G. Snyder, and J. A. Woollam, *J. Vac. Sci. Technol. A* **11**, 1075 (1993).
- ²⁸E. O. Goebel, *Springer Proceedings in Physics*, Vol. 25 (Springer, Berlin, 1988), p. 204.
- ²⁹D. E. Aspnes, S. M. Kelso, R. A. Logan, and R. Bhat, *J. Appl. Phys.* **60**, 754 (1986).
- ³⁰M. Nido, M. G. W. Alexander, W. W. Rühle, T. Schweizer, and K. Köler, *Appl. Phys. Lett.* **56**, 355 (1990).
- ³¹R. Eccleston, R. Strobel, J. Kuhl, and K. Köler, *International Meeting on Optics of Excitons in Confined Systems*, *Inst. Phys. Conf. Ser. No. 123* (IOP, Bristol, 1992).
- ³²F. Evangelisti, A. Frova, and J. U. Fischbach, *Surf. Sci.* **37**, 841 (1973); F. Evangelisti, J. U. Fischbach, and A. Frova, *Phys. Rev. B* **9**, 1516 (1974).
- ³³F. Martelli, M. Capizzi, A. Frova, A. Polimeni, F. Sarto, M. R. Bruni, and M. G. Simeone, *Phys. Rev. B* **48**, 1643 (1993).
- ³⁴J. Kusano, Y. Aoyagi, S. Namba, and H. Okamoto, *Phys. Rev. B* **40**, 1685 (1989).
- ³⁵Ph. Roussignol, C. Delalande, A. Vinattieri, L. Carraresi, and M. Colocci, *Phys. Rev. B* **45**, 6965 (1990).
- ³⁶T. C. Damen, J. Shah, D. Y. Oberli, D. S. Chemla, J. E. Cunningham, and J. M. Kuo, *J. Lumin.* **45**, 181 (1990).
- ³⁷E. S. Aydil, Z. Zhou, K. P. Giapis, Y. Chabal, J. A. Gregus, and R. A. Gottscho, *Appl. Phys. Lett.* **62**, 3156 (1993).
- ³⁸K. C. Hsieh, M. S. Feng, G. E. Stillman, N. Holonyak, Jr., C. R. Ito, and M. Feng, *Appl. Phys. Lett.* **54**, 341 (1989).
- ³⁹Capasso and G. F. Williams, *J. Electrochem. Soc.* **129**, 821 (1982).
- ⁴⁰L. Sorba, M. Pedio, S. Nannarone, S. Chang, A. Raisanen, A. Wall, P. Philip, and A. Franciosi, *Phys. Rev. B* **41**, 1100 (1990).
- ⁴¹F. Proix, *Physica B* **170**, 457 (1991), and references therein.
- ⁴²D. J. Frankel, J. Anderson, G. J. Lapeyre, and H. H. Farrell, *J. Vac. Sci. Technol. B* **3**, 1093 (1985).
- ⁴³Th. Allinger, J. A. Schaefer, C. Stuhlmann, U. Beckers, and H. Ibach, *Physica B* **170**, 481 (1991).
- ⁴⁴D. Liu, T. Zhang, R. A. LaRue, J. S. Harris, Jr., and T. W. Sigmon, *Appl. Phys. Lett.* **53**, 1059 (1988).
- ⁴⁵A. Amore Bonapasta (private results from local density approximation).
- ⁴⁶J. Lagowski, M. Kaminska, J. M. Parsey, Jr., H. C. Gatos, and M. Lichtensteiger, *Appl. Phys. Lett.* **41**, 1078 (1982); E. M. Omel'yanovskii, A. V. Pakhomov, and A. Ya. Polyakov, *Sov. Phys. Semicond.* **21**, 514 (1987).